Journal of Applied Polymer Science

Orientation of HDPE Inclusions Within Solid-State Drawn Rubber-Modified Isotactic Polypropylene: DSC Insight

Marta Slížová,[1] Miroslav Raab[2]

[1]Department of Physics and Materials Engineering, Faculty of Technology, Tomas Bata University in Zlin, Nad Stranemi 4511, 760 05 Zlin, Czech Republic

[2]Institute of Macromolecular Chemistry, AS CR, v.v.i., Heyrovsky Sq. 2, 162 06 Prague 6, Czech Republic

Correspondence to: M. Slížová (E-mail: slizova@ft.utb.cz)

ABSTRACT: Effect of drawing temperature on the melting behavior of oriented isotactic polypropylene (PP) modified with ethylene-propylene-diene monomer rubber with a small amount of high-density polyethylene (HDPE) is explored in this study. Injection-molded specimens both neat and 8 vol % modified PP were solid-state drawn to natural drawing ratio and characterized by X-ray diffraction, dynamic mechanical analysis (DMA), Charpy impact test and differential scanning calorimetry (DSC). A synergy of orientation and embedding rubber particles caused a significant increase of low-temperature notched impact strength of oriented blends. It was shown, that the DSC method can be used successfully for the indirect but very sensitive characterization of orientation on a nanometre scale. At the drawing temperature of 120°C, the DSC data indicated an incomplete transition of the PP crystalline structure: This is reflected by splitting and shifting of the melting peak of PP. An increase of the melting temperature of the HDPE inclusions by 3.5°C reflects the high orientation. © 2013 Wiley Periodicals, Inc. J. Appl. Polym. Sci. 130: 603–609, 2013

KEYWORDS: blends; differential scanning calorimetry; structure-property relations; polyolefins; orientation

Received 5 October 2012; accepted 22 February 2013; published online 20 March 2013

DOI: 10.1002/app.39207

INTRODUCTION

Isotactic polypropylene (PP) is the fastest growing commodity plastic because of a very favorable price/performance ratio and a successful tailoring the end-use properties. Its low toughness at lower temperatures has been overcome by blending with ethylene-propylene-diene monomer (EPDM) rubbers. Some producers used more complex toughening additives containing both EPDM rubber and high-density polyethylene (HDPE). It has been suggested, that small amount of HDPE further enhances the material toughness. Additionally, it improves interface adhesion and miscibility. Several authors have studied dynamic mechanical properties and impact resistance of these complex materials.[1–7] The impact-resistant PP or copolymer PP can be produced effectively by *in situ* copolymerization with ethylene. These multiphase materials contain PP matrix and dispersed ethylene-propylene random copolymer (EPR) droplets with the crystalline PE-rich core and the crystalline PP-rich layer around EPR shell.[8,9]

Morphology of the impact rubber modified PP can be studied by X-ray diffraction, light scattering, differential scanning calorimetry (DSC), and microscopy.[10–13] Typically a shell–core structure of toughening particles is formed with PE in the core and EPDM layer forming the shell. EPDM cover of PE core is more or less perfect. In these cases, a specific flake structure of toughening particles was described.[14] In fact, injection-molding technology itself can produce elongated EPDM particles in PP.[15] In our case, however, the original elongation of the particles (before drawing) was not significant. According to our previous studies, diameters of the embedded EPDM/HDPE particles are less than 0.6 μm for low concentrations.[16,17]

Several authors studied the transformation of modified PP during solid-state drawing and interactions between drawing conditions and macroscopic impact resistance.[14,16–18] It was proved, that the presence of rubber influences the efficiency of drawing and the resulting morphology. During drawing, rubber inclusions are oriented in drawing direction, but macroscopic drawing ratio is slightly lower in comparison with PP matrix.[13,17] dynamic mechanical analysis (DMA) curves of oriented blends show disappearance of the typical relaxation peak at glass temperature region of EPDM.[18] Also, PP-based materials drawn at elevated temperatures show high impact resistance, even at cryogenic temperatures.[19] This study is aimed at melting behavior of PP modified by 8 vol % EPDM, drawn at various temperatures. For comparison, results for neat PP were also discussed.

Table I. Composition of Original Materials

Code	PP matrix	EPDM modifier	EPDM (vol %)	HDPE (vol %)	MFI (g/10 min) [230°C, 21.12 N]
PP	Mosten 58412[a]	-	0	0	3.0-4.0
MD	Mosten 58412[a]	Dutral TP50F	5.6	2.4	2.5-4.0
TD	Tatren PF/M[b]	Dutral TP50F	5.6	2.4	8.5-11.0

[a]Produced by Chemopetrol, Litvínov, Czech Republic.8, [b]Produced by Slovnaft Petrochemicals, Bratislava, Slovakia.

Table II. Yield Stress σ_Y(MPa) of Neat and Rubber Modified PP for Different Drawing Temperatures

	Yield stress σ_Y (MPa)					
T_D (°C)	60	100	110	120	130	150
PP	16.0 ± 0.9	10.3 ± 1.2	7.5 ± 0.3	6.0 ± 0.9	4.0 ± 0.5	2.5 ± 0.8
MD	8.9 ± 1.0	9.0 ± 2.0	8.0 ± 0.5	7.3 ± 0.9	-	2.3 ± 0.5
TD	9.0 ± 0.9	8.5 ± 1.0	7.1 ± 0.5	6.1 ± 0.4	-	2.8 ± 0.5

EXPERIMENTAL

Materials

Experimental samples of isotactic PP, both neat and modified by 8 vol % EPDM rubber with HDPE were selected as starting materials throughout this study. The composition and characterization of the samples are summarized in Table I.

From the pellets of the basic materials, standard dumbbell specimens were prepared by injection-molding, under these conditions: the temperatures of heating zones were 210, 220, 230, and 230°C, the temperature of mold of 60°C and the injection pressure of 37.5 MPa.

All tensile specimens were exposed to drawing at temperature range from 60 to 150°C. Instron tester equipped with temperature cabinet was used for the drawing experiments. The specimens were drawn at the rate of 20 mm/min to maximum strain given by the inner space of temperature cabinet and slowly relaxed under stress 24 h at ambient temperature. The samples were drawn to their natural drawing ratio.[20] The natural drawing ratio was determined from equidistant markers on the surface of the sample. As the natural drawing ratio does not depend significantly on the drawing temperature, only average values have been indicated. The central part of drawn samples about 90 × 5 × 1.8 mm^3 has been used for the next evaluation. For each drawing temperature and material, three to five samples were taken.

Methods

Instron 1122 tester equipped with temperature cabinet Instron 3100 was used for the solid state drawing.

WAXD difractograms of drawn samples were recorded with difractometer Micrometa 2E. Average sizes of crystalline zones L_{111}, L_{010} in directions perpendicularly to the reflection planes (111), (010) were determined by using Scherrer equation.[21] A Kratki camera (A. Paar, Austria) was employed for SAXS measuremensts. Peak positions on Lorentz-corrected scattering curves were employed to obtain the long period (LP) values according to Bragg's law.[21] In X-ray experiments, monochromatic CuK_α radiation of wavelenght 0.154 nm was used.

Notched impact strength was determined on Charpy pendulum at −70°C according to Ref. 19. Each measurement was repeated five times and average values reported. Experimental scatter of the measuremens was about 20%.

For DMA, an instrumented free-oscilating torsion pendulum with liquid nitrogen cooling was used at temperature range from −130 to 20°C. Rectangular specimens (80 × 5 × 1.8 mm^3) were tested at 1 Hz.

DSC Perkin-Elmer 4 was used for thermal analysis. The samples of about 5 mg were taken from the central part of the injection-molded and/or drawn specimens. These tested samples were heated from 60 to 200°C at the rate of 10 K/min. For each

Table III. Comparison of SAXS, WAXD Morphology Parameters of Drawn Samples

T_D (°C)	60		100		110	120	150	
Material	PP	MD	PP	MD	PP	PP	PP	MD
LP (10^{-10} m)	129	128	178	169	196	206	330	280
L_{111} (10^{-10} m)	129	89	148	115	149	162	205	191
L_{110} (10^{-10} m)	36	87	88	98	93	100	125	157

Table IV. Charpy Notched Impact Strength a_n (kJ/m^2) Measured at −70°C

	Charpy notched impact strength a_n (kJ/m^2)					
T_D (°C)	-	60	100	110	120	150
PP	3.8 ± 0.4	160 ± 15	140 ± 30	150 ± 20	140 ± 30	180 ± 10
MD	3.7 ± 0.3	140 ± 20	120 ± 15	200 ± 20	200 ± 20	100 ± 25
TD	4.3 ± 0.5	110 ± 10	150 ± 30	170 ± 30	120 ± 15	100 ± 10

materials, 5–10 samples were tested and the results statisticaly evaluated. The heat of fusion of HDPE reflects its small portion in the whole sample (2.4 vol %). The expression of PE content in wt % is not possible as the modifier contained also amorphous EPDM.

RESULTS AND DISCUSSION

Stress–Strain Behavior of Original Injection-Molded Materials

Values of yield stress attained from stress–strain curves for neat and modified PP at elevated temperatures are presented in Table II. Yield stress decreases with increasing drawing temperature (T_D) for all drawn materials. At the same time, the macroscopic natural drawing ratio of central part of samples was 5.5 ± 0.3 for neat PP, 6.0 ± 0.2 for the blend MD and 6.4 ± 0.4 for TD, respectively. Effect of drawing temperature on natural drawing ratio was not statistically significant. All materials deformed nonuniformly showing localized necking and stress-whitening.[22] Stress-whitening decreased significantly above T_D 120°C.[13,17]

Structure, Impact Behavior, and DMA

For a more detailed comparison of drawn neat and modified materials, SAXS, WAXD, and −70°C Charpy notched impact strength data of selected oriented samples are summarized in Tables III and IV. During solid-state drawing, transition from lamellar (spherulitic) to fibrillar morphology takes place in the propagating neck shoulder.[23,24] In samples drawn to the natural drawing ratio, fibrils contain crystalline and amorphous zones with macromolecules strongly oriented in the direction of drawing.[25,26]

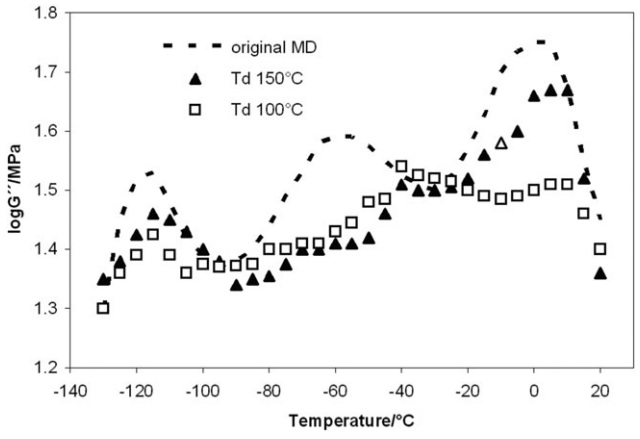

Figure 1. DMA spectra of original and oriented MD blends: Loss modulus G''.

SAXS and WAXD methods provide spatial information over size scales about units up to 10 nm.[27,28] LP from SAXS data represents the most probable distance of centers of gravity of two adjacent lamellae, including amorphous phase. LP of drawn samples was determined along the direction of drawing. Perpendicularly, no periodicity occurred. Values of LP (Table III) are increasing with increasing drawing temperature for all materials. The marked increase is shown above T_D of 120°C.

Crystall lamellae thicknesses can be estimated by analysis of WAXD difractogrames. The lateral size L_{110} of crystalline zones of oriented PP is measured perpendicularly to crystalline *c*-axis, that is, chain axis, respectively. A reflection plane (111) is inclined in relation to the surface of lamellae therefore L_{111} size can introduce approximately longitudinal thickness of PP crystallites. It has been found that crystalline domains of modified PP are shorter but broader then in neat PP. In materials oriented above T_D of 120°C, comparison of L_{111} thickness and LP shows significant effect of amorphoes phase in transformed fibrils.

The Charpy impact strength shows a maximum for characteristic T_D depending on the sample composition (Table IV). All oriented specimens showed a typical hinge break.[19] Significant splitting along the drawing direction occurred in the case of neat PP only. Conversely, rubber-modified PP blends are significantly more impact resistant due to Cook Gordon mechanism of multiple effective crack blunting[19] and synergy effect of orientation and rubber modification is evident.

Temperature dependences of loss modulus G'' for original and drawn blends are presented in Figure 1. Loss modulus reflects marked changes of morphology in drawn blends. A low-temperature relaxation of HDPE and EPDM at about −115°C becomes lower by drawing. This can indicate reduced mobility of short molecular segments due to orientation.[18] Disappearance of a relaxation peak at glass temperature of EPDM is evident for drawn.[18] Relaxation peak at the glass temperature region of PP is affected by drawing and reflects higher orientation of PP amorphous phase at lower T_D. The same trend was found for TD blend.

Melting Behavior of Materials Drawn at Various Temperatures

Selected DSC curves of the original neat PP and the corresponding drawn specimens are shown in Figure 2. Typical melting peak of original PP is located at a temperature of 163.8 ± 0.9°C, corresponding heat of fusion is of 76 ± 4 J/g. Statistical evaluation includes undrawn samples, annealed at drawing temperatures in Instron cabinet. Results for the drawn specimens

Applied Polymer SCIENCE

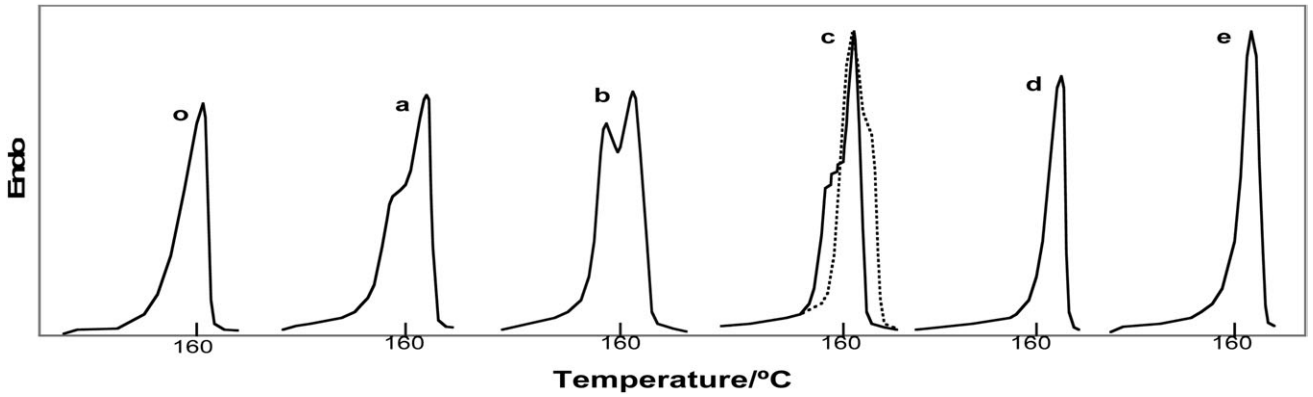

Figure 2. DSC curves of original (o) and drawn PP: drawing temperatures a—60°C, b—100°C, c—120°C, d—130°C, e—150°C.

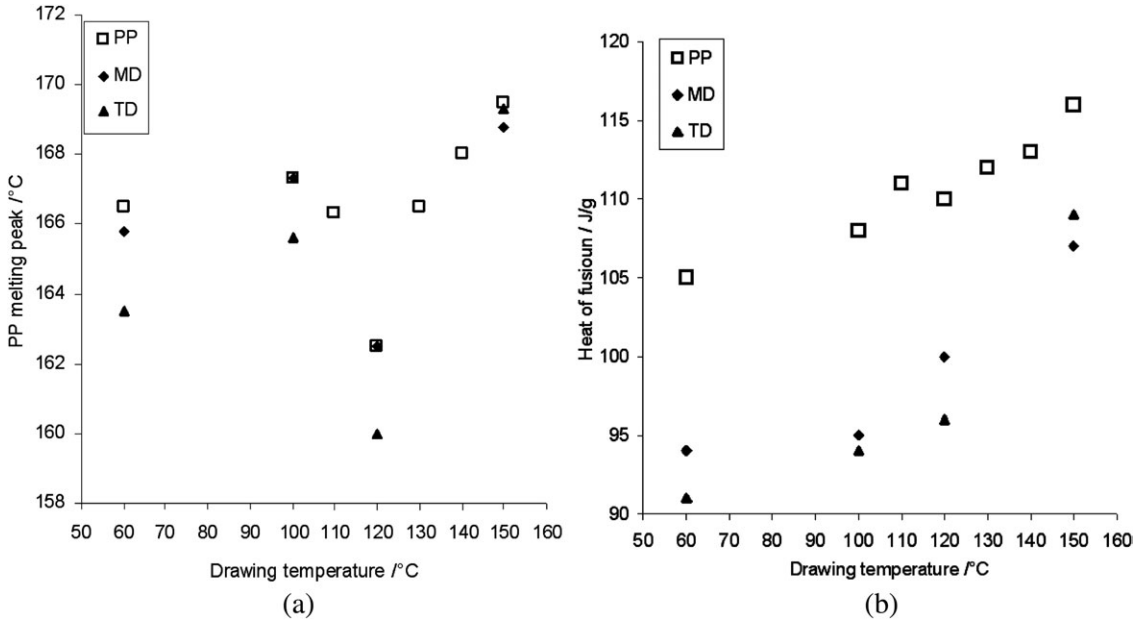

Figure 3. The effect of drawing temperature (a) on the position of the PP melting peak (b) on the heat of fusion for drawn neat and rubber modified PP.

show a splitting of the melting maximum.[24,25] It might suggest a formation of two different crystalline structures. With increasing T_D, only one melting peak occurs, but its maximum is shifted to higher temperatures. For drawn samples, an increase of heat of fusion by nearly 30% shows that crystallinity is affected by drawing dramatically [Figure 3(b), empty squares].

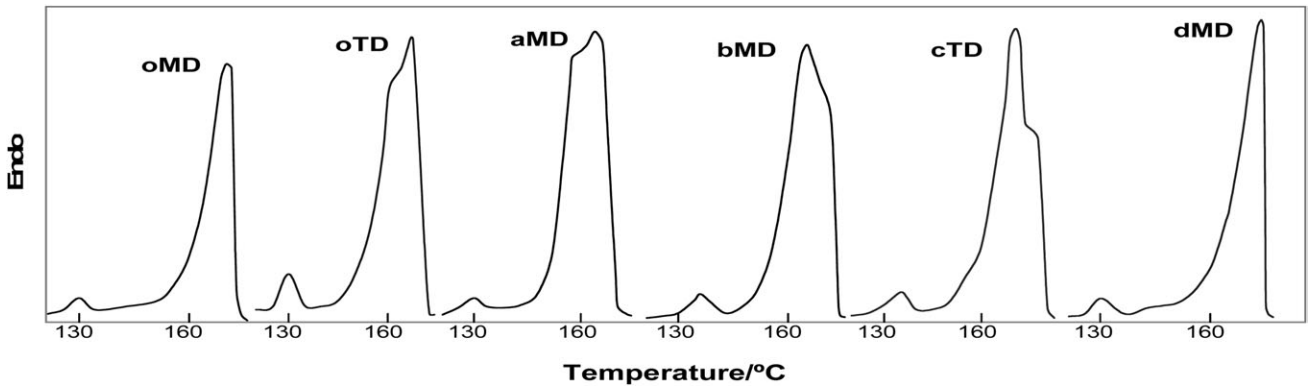

Figure 4. DSC curves of original (o) and drawn blends MD and TD for drawing temperatures a—100°C, b—120°C, c—120 °C, d—150°.

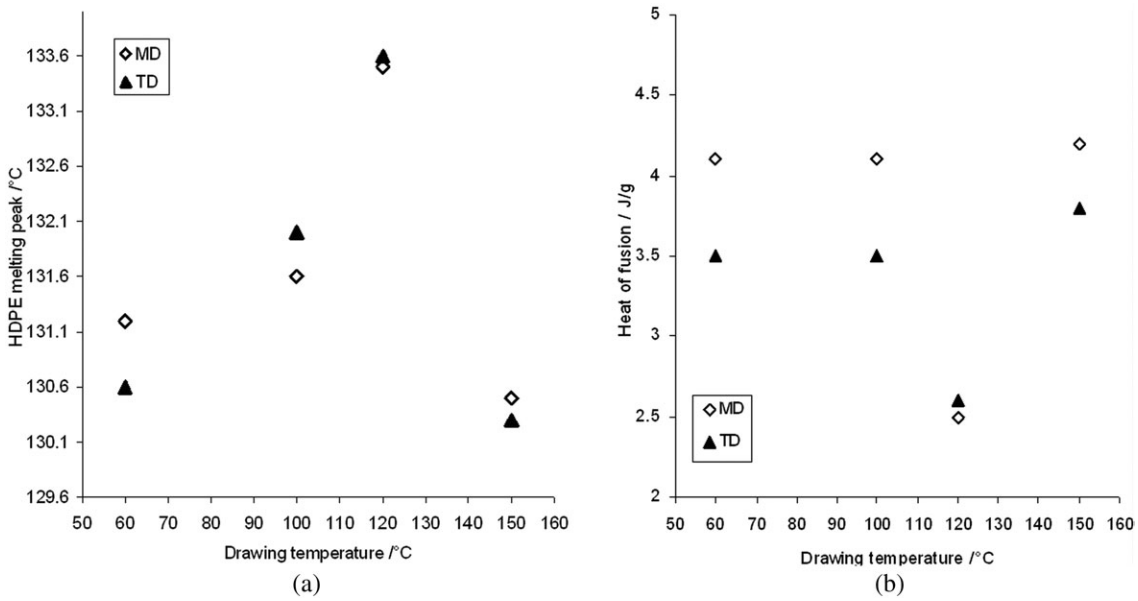

Figure 5. The effect of drawing temperature (a) on the position of the PE melting peak, (b) on the heat of fusion for HDPE.

The location of the main melting maximum (T_{mPP}) of oriented PP shows a deep drop to 162.5 ± 0.3°C at a critical drawing temperature of 120°C [Figure 3(a), empty squares] and this value is similar to a undrawn sample with the same thermal history, 162.9 ± 0.5°C. The endothermic peaks are more complex with shoulders under or above T_{mPP}. The marked decrease of T_{mPP} could be ascribed to a disruption and an incomplete transition of crystalline PP during solid-state drawing. It should be noted that LP increased (Table III), but heat of fusion slightly decreased at T_D of 120°C in comparison with the most effective T_D of 110°C [17] [Figure 3(b)]. Indeed, the splitting of DSC curves reflects formation of less perfect crystalline zones in fibrils oriented at 120°C [17]. Melting temperature and heat of fusion are increasing more significantly at higher drawing temperatures. Under these conditions, annealing is more effective and bigger crystalline domains can appear in fibrils.

DSC curves of two blends modified by rubber and HDPE are shown in Figure 4. These PP blends contain the same concentration of identical modifier, but differ in the PP matrix. PP melting temperatures T_{mPP} and heats of fusion of original blends differed, but slightly: 165.1 ± 0.3°C, 75 ± 2 J/g for MD and 163.0 ± 0.2°C, 73 ± 2 J/g for TD, respectively. Not surprisingly, no distinct melting peak that would correspond to the rubber portion appeared on the curves. It indicates that the EPDM rubber was fully amorphous in both cases above the starting temperature of the DSC measurement (60°C).[29] In both oriented blends, T_{mPP} decreases at T_D of 120°C similarly as for the neat PP [Figure 3(a), rhombuses, triangles].

In original specimens, the distinct melting HDPE peak T_{mPE} is located at 130.1 ± 0.1°C. The T_{mPE} of 130°C was repeatedly detected for both MD and TD blends. The shift from a standard 133°C could be ascribed to smaller dimensions of PE droplets and is typical for PP/HDPE blends with low concentrations of HDPE.[30]

The location of the HDPE peak increased slightly but significantly with increasing T_D [Figure 5(a)], melting peaks are broader than those of nonoriented samples [Figure 6(a,b)]. At drawing temperature of 120°C, T_{mPE} reaches 133.6 ± 0.2 °C for both blends and decreases again at T_D of 150°C, which is above the HDPE melting temperature. In this case, HDPE can melt and recrystallize during drawing [Figure 5(a)]. On the other hand, crystallinity is lower at T_D of 120°C [Figure 5(b)]. It can be suggested that the portion of HDPE is highly oriented, but not crystallized. Important noticing, variation of PP matrix had no essential effect on the melting behavior of HDPE inclusions [Figure 6(a,b)].

It should be referred that Cappacio and Ward found 118–120°C as an optimum temperature interval for effective orientation of HDPE.[31] It is generally known that HDPE melting temperature increases with an increasing drawing ratio and location of the melting peak is connected with the orientation of the amorphous phase of polymer.[32] In the case of the PP blends, the PE inclusions indicate that the critical drawing temperature of 120°C corresponds to the optimum orientation drawing of PE and can be interpreted as a temperature of balance between molecular mobility and localized viscosity. At the same time, it is demonstrated here that small domains of crystalline PE sensitively reflect conditions of orientation drawing on nanometre scale and can serve as a probe of localized orientation. In our opinion, this approach can be applied for other materials based on PP, especially for multiphase impact PP copolymers.[8,9]

CONCLUSIONS

Neat PP and two samples of PP modified by EPDM rubber with small amount of HDPE were exposed to solid-state

Applied Polymer SCIENCE

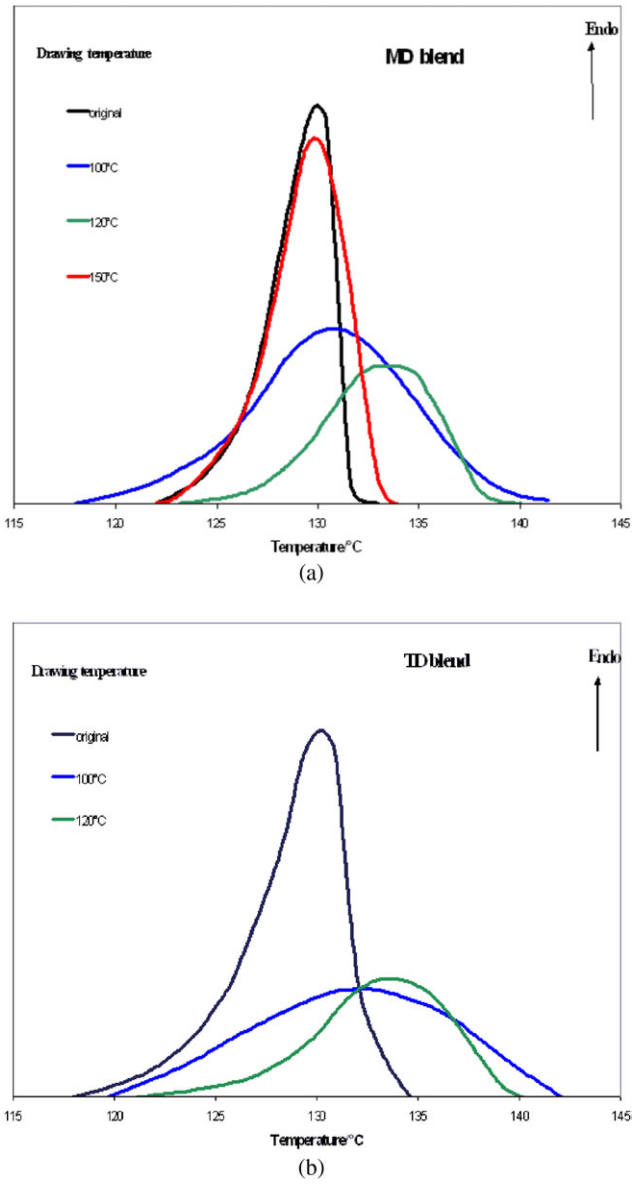

Figure 6. Insets of DSC curves of the HDPE inclusions in original and oriented blends (a) MD, (b) TD. [Color figure can be viewed in the online issue, which is available at wileyonlinelibrary.com.]

drawing. Oriented materials showed an improved toughness and impact resistance perpendicular to the drawing direction. The synergy effect of orientation and EPDM/HDPE modification caused the increasing low-temperature notched impact strength of these oriented blends above the values of neat oriented PP.

The PP-melting peak location in all oriented materials has shown a marked drop at drawing temperature of 120°C indicating disruption of crystalline structure during drawing and forming different crystalline zones. The broadenig of the DSC peak of PP could be attributed to imperfect formation of crystalline zone in oriented fibrils during drawing. This notion corresponds to commonly accepted models.[17,26]

A small but distinct peak of HDPE has shown an increase from 130.1 to 133.6°C for materials drawn at 120°C. This result corresponds to the optimum drawing temperature already found for neat HDPE.[31] Thus, DSC method can be used for indirect but sensitive characterization of localized orientation using of HDPE particles as a probe on nanometre scale.

REFERENCES

1. Kolařík, J.; Velek, J.; Agarval, G. L.; Fortelný, I. *J. Polym. Comp.* **1998**, *7*, 472.
2. Hemmati, M.; Nasokdast, H.; Shariat Panahi H. *J. Appl. Polym Sci.* **2001**, *82*, 1138.
3. Tchomakov, K. P.; Favis, B. D.; Huneault, M. A.; Champagne, M. F.; Tofan, F. *Can. J. Chem. Eng.* **2005**, *83*, 300.
4. Mohanraj, J.; Chapleau, N.; Ajji, A.; Ducket, R. A.; Ward, I. M. *J. Polym. Eng. Sci.* **2003**, *43*, 1317.
5. Vranjes, N.; Rek, V. *Macromol. Symp.* **2007**, *258*, 90.
6. Huang, H.-J.; Yang, W.; Xie, B.-H.; Li, Q.-G.; Yang, M.-B. *J.Elast. Plast.* **2010**, *40*, 75.
7. Bárány, T.; Czigány, T.; Karger-Kocsis, J. *Prog. Polym. Sci.* **2010**, *35*, 1257.
8. van Reenen, A. J.; Basson, N. C. *Express Polym. Lett.* **2012**, *6*, 427.
9. Luo, F.; Xu, CL.; Wang, Ch.; Deng, H.; Chen, F.; Fu, Q. *Polymer*, **2012**, *53*, 1783.
10. Hemmati, M.; Nasokdast, H.; Shariat Panahi, H. *J. Appl. Polym. Sci.* **2001**, *82*, 1129.
11. Nedkov, T.; Lednický, F, Mihailova, M. *J.Appl. Polym. Sci.* **2008**, *109*, 226.
12. Na, B.; Wang K.; Zhang, Q.; Du, R.; Fu, Q. *Polymer* **2005**, *46*, 3190.
13. Holoubek, J.; Kotek J.; Raab M. *Polym. Bull.* **1996**, *37*, 631.
14. Nedkov, T.; Lednický, F. *J. Appl. Polym. Sci.* **2003**, *90*, 3087.
15. Karger-Kocsis, J. *Polym. Eng. Sci.* **1987**, *27*, 241
16. Holoubek, J. *Polymer* **1999**, *40*, 277.
17. Kotek, J.; Ščudla, J.; Šlouf, J.; Raab, M. *J. Appl. Polym. Sci.* **2007**, *103*, 3539.
18. Amash, H.; Zugenmaier P. *J. Polym. Sci. Polym. Phys.* **1997**, *35*, 1439.
19. Sova, M.; Raab, M.; Sližová M. *J. Mater. Sci.* **1993**, *28*, 6516.
20. Seguella, M. *Macromol. Mater. Eng.* **2007**, *292*, 235.
21. Kotek, J.; Raab, M.; Baldrian J, Grellmann, W. *J. Appl. Polym. Sci.* **2002**, *85*, 1174–1184.
22. Karger-Kocsis, J.; Wanjale, S. D.; Abraham, T.; Bárány, T.; Apostolov, A. A. *J. Appl. Polym. Sci.* **2010**, *115*, 684.
23. Nouzue, Y.; Shinohara, I.; Ogawa, I.; Samuraj, T.; Hori, H.; Kasahara, T.; Yamaguchi, N.; Yagi, N.; Amemiya, I. *Macromolecules* **2007**, *40*, 2036.
24. Kratochvíl, J.; Kotek, J, Sikora, A.; Raab, M. *Macromol. Symp.* **1999**, *147*, 155.

25. Ščudla, J.; Eichhorn K. Raab, M.; Schmidt, P.; Jehnichen, D, Haussler, L. *Macromol. Symp.* **2002**, *181*, 371.
26. Schmidt, P.; Baldrian, J.; Ščudla, J.; Dybal, J.; Raab, M.; Eichhorn, K. *Polymer* **2001**, *42*, 5321.
27. Ran, S.; Zong, X.; Fang, D.; Hsiao, B. S.; Chu, B.; Philips, A. R. *Macromolecules* **2001**, *40*, 2569.
28. Machado, G.; Kanast, J. E.; Scholten, D. J.; Thompson, A.; De Vargas, T.; Teixiera, S. R.; Samos, D. *Eur. Polym. J.* **2009**, 45, 700.
29. Scholtens, B. J. R, Riande, E.; Mark, J. E. *J. Polym. Sci. Polym. Phys.* **1984**, *22*, 1223.
30. Marossi, G.; Anna, P.; Bertalan, G.; Tohl, A.; Lágner, P.; Balogh, I.; Papp, I. *J. Thermal Analysis* **1996**, *47*, 463.
31. Capaccio, G.; Crompton, A.; Ward, I. M. *J. Polym .Sci. Polym. Phys.* **1979**, *18*, 301.
32. Meinel, G.; Peterlin, A. *J. Polym. Sci. Polym. Phys* **1968**, *6*, 587.